

Inference on testing the number of spikes in a high-dimensional generalized spiked Fisher matrix

Rui Wang¹ and Dandan Jiang^{1,*}

¹*School of Mathematics and Statistics, Xi'an Jiaotong University, Xi'an, China*
e-mail: wangrui_math@stu.xjtu.edu.cn; jiangdd@mail.xjtu.edu.cn

Abstract: The spiked Fisher matrix is a significant topic for two-sample problems in multivariate statistical inference. This paper is dedicated to testing the number of spikes in a high-dimensional generalized spiked Fisher matrix that relaxes the Gaussian population assumption and the diagonal constraints on the population covariance matrices. First, we propose a general test statistic predicated on partial linear spectral statistics to test the number of spikes, then establish the central limit theorem (CLT) for this statistic under the null hypothesis. Second, we apply the CLT to address two statistical problems: variable selection in high-dimensional linear regression and change point detection. For each test problem, we construct new statistics and derive their asymptotic distributions under the null hypothesis. Finally, simulations and empirical analysis are conducted to demonstrate the remarkable effectiveness and generality of our proposed methods across various scenarios.

MSC2020 subject classifications: Primary 62H15; secondary 62H10.

Keywords and phrases: High-dimensional data, generalized spiked Fisher matrix, testing the number of spikes, central limit theorem.

Contents

1	Introduction	2
2	Testing the number of spikes for a generalized spiked Fisher matrix	4
	2.1 Model formulation	4
	2.2 Test on the number of spikes: the general case	5
	2.3 The low-rank case of $\Sigma_1 - \Sigma_2$	7
3	Application to large-dimensional linear regression models	9
4	Application to change point detection	12
5	Numerical and empirical studies	14
	5.1 Evaluation for the CLT proposed in Theorem 2.1	14
	5.2 Numerical studies for large-dimensional linear regression	17
	5.3 Numerical studies for change point detection	19
	5.4 Empirical study	21
6	Conclusion	22
A	Proof of Theorem 2.1	23
	Acknowledgments	25

*Corresponding author: Dandan Jiang.

Funding	25
Supplementary Material	25
References	25

1. Introduction

The spiked model, initially introduced by [13], describes that some extreme eigenvalues of random matrices exhibit significant separation from the remainder. This model plays a pivotal role in multivariate statistical inference and has a wide range of applications in many modern fields, such as wireless communication [21, 10], speech recognition [7, 13], and other scientific fields. A critical aspect of the spiked model is to determine the number of spiked-eigenvalues (spikes), which helps reveal the latent dimensionality of data and the underlying structure of the population. Notably, due to the close relationship between the spiked model and principal component analysis (PCA), and factor analysis (FA), determining the number of principal components (PCs) or factors is equivalent to finding the number of spikes.

Numerous studies have been devoted to this topic in one-sample spiked population models. One prominent type of research focuses on information criteria, such as [3], which developed a constructive work to provide several information criteria for estimating the number of factors. Following their work, [16, 1, 18] et al. improved these criteria using different tools. Another main type of research relies on the asymptotic behavior of eigenvalues. The reference [15] estimated the number of PCs by comparing the sample eigenvalues against a threshold derived from the Tracy-Widom Law. Alternatively, [19] and [20] developed approaches based on differences in consecutive sample eigenvalues. More recently, [9] proposed a partial linear spectral statistic to test the number of spikes in generalized spiked covariance matrices. Despite these advancements, the studies on determining the number of spikes for two-sample spiked models has received less attention.

The two-sample spiked model addresses the problems involving two p -dimensional populations with covariance matrices Σ_1 and Σ_2 . When the matrix $\Sigma_1 \Sigma_2^{-1}$ possesses a few extreme eigenvalues that are significantly distinct from the remaining ones, the Fisher matrix $\mathbf{S}_1 \mathbf{S}_2^{-1}$ is called the spiked Fisher matrix, where \mathbf{S}_1 and \mathbf{S}_2 are the corresponding sample covariance matrices. Determining the number of spikes in such a two-sample spiked model was initially studied in [23] with a simple formation of

$$\Sigma_1 = \Sigma_2 + \Delta, \quad (1)$$

where Δ is a symmetric matrix with low rank. In their study, [23] compared the sample eigenvalues against a threshold in a similar way to [15]. However, when $\Sigma_1 \Sigma_2^{-1}$ satisfies the condition in (1), it inherently has equal non-spiked eigenvalues of 1, thereby restricting its applications to more complex covariance structure. Subsequently, motivated by the hypothesis testing problem $\mathcal{H}_0 : \Sigma_1 = \sigma^2 \Sigma_2$ v.s. $\mathcal{H}_1 : \Sigma_1 = \sigma^2 \Sigma_2 + \Delta$, [24] explored a more general spiked Fisher

matrix, where the non-spiked eigenvalues are still assumed to be identical. They introduced a generic criterion to estimate the number of spikes, later extended by [25] to scenarios where the number of spikes diverges as p goes to infinity. Nevertheless, all of these models are unsuitable for more complex structures characterized by varying non-spiked eigenvalues. This leads to the study of the so-called generalized spiked Fisher matrix, as investigated in [11] and [6], where $\Sigma_1 \Sigma_2^{-1}$ has the spectral form

$$\underbrace{\alpha_1, \dots, \alpha_1}_{m_1}, \dots, \underbrace{\alpha_K, \dots, \alpha_K}_{m_K}, \beta_{p, M+1}, \dots, \beta_{p, p}. \quad (2)$$

Here, the spectrum in (2) is arranged in descending order, where $\alpha_1, \alpha_2, \dots, \alpha_K$ are spikes with multiplicity m_1, m_2, \dots, m_K , satisfying $m_1 + m_2 + \dots + m_K = M$ with M being a fixed integer. These spikes are significantly larger than the remaining non-spiked eigenvalues $\beta_{p, M+1}, \dots, \beta_{p, p}$.

In this paper, we focus on testing the number of spikes in a generalized spiked Fisher matrix, as described in (2), when both the sample size and the dimension of variables proportionally tend to infinity. We first propose a general test statistic that relies on a partial linear spectral statistic, and establish its asymptotic normality under the null hypothesis. This test is then applied to two statistical problems: testing the number of significant variables in a large-dimensional linear regression model and testing the change points in the sequence data. Our approach offers several notable advantages compared to existing works. Firstly, our method exhibits superior generality as it is free of population distributions of samples, and does not rely on the diagonal assumption of the population covariance matrices. Furthermore, the proposed method is more comprehensive with general assumptions of Σ_1 and Σ_2 , and encompasses the low-rank case of $\Sigma_1 - \Sigma_2$ as a special instance. Finally, beyond theoretical advancements, our practical applications demonstrate commendable performance. In the variable selection problem for large-dimensional linear regression, our test accurately identifies the number of significant variables, exhibiting correct sizes and robust behavior. Additionally, in the change point detection problem, our method consistently achieves higher accuracy across various scenarios compared to existing approaches.

The arrangement of this article is as follows. Section 2 introduces the generalized spiked Fisher matrix, proposes a test for the number of spikes, and derives its asymptotic normality under the null hypothesis. Following this, Section 3 and Section 4 elaborate on two practical applications of the proposed test, the identification of the number of significant variables in the large-dimensional linear regression model and the change point detection. Section 5 conducts numerical and empirical studies for the above results. Finally, Section 6 offers concluding remarks. Proofs are provided in the appendix.

2. Testing the number of spikes for a generalized spiked Fisher matrix

2.1. Model formulation

Following [11], the generalized spiked Fisher matrix serves as the primary target matrix for the statistical problems within the two-sample spiked model, which is formulated as follows. Let $\mathbf{\Sigma}_1$ and $\mathbf{\Sigma}_2$ be two general independent and deterministic matrices, where $\mathbf{\Sigma}_1$ is non-negative definite, and $\mathbf{\Sigma}_2$ is positive definite. To begin with, we define

$$\begin{aligned}\mathbf{X} &= (\mathbf{x}_1, \mathbf{x}_2, \dots, \mathbf{x}_{n_1}) = (x_{ij}, 1 \leq i \leq p, 1 \leq j \leq n_1), \\ \mathbf{Y} &= (\mathbf{y}_1, \mathbf{y}_2, \dots, \mathbf{y}_{n_2}) = (y_{il}, 1 \leq i \leq p, 1 \leq l \leq n_2),\end{aligned}$$

where $\{x_{ij}, i, j = 1, 2, \dots\}$ and $\{y_{il}, i, l = 1, 2, \dots\}$ are either both real or both complex random variable arrays, satisfying the following assumption.

Assumption 1. The two independent double arrays $\{x_{ij}, i, j = 1, 2, \dots\}$ and $\{y_{il}, i, l = 1, 2, \dots\}$ are independent and identically distributed (i.i.d.) random variables with mean 0 and variance 1. $E(x_{ij}^2) = E(y_{ij}^2) = 0$ for the complex case. Moreover, $E|x_{ij}|^4 < \infty$ and $E|y_{ij}|^4 < \infty$.

Given this assumption, $\mathbf{\Sigma}_1^{1/2}\mathbf{X}$ and $\mathbf{\Sigma}_2^{1/2}\mathbf{Y}$ can be seen as two independent random samples from the p -dimensional populations with general population covariance matrices $\mathbf{\Sigma}_1$ and $\mathbf{\Sigma}_2$, respectively. The corresponding sample covariance matrices of the two observations are given by

$$\mathbf{S}_1 = \frac{1}{n_1} \mathbf{\Sigma}_1^{\frac{1}{2}} \mathbf{X} \mathbf{X}^* \mathbf{\Sigma}_1^{\frac{1}{2}} \quad \text{and} \quad \mathbf{S}_2 = \frac{1}{n_2} \mathbf{\Sigma}_2^{\frac{1}{2}} \mathbf{Y} \mathbf{Y}^* \mathbf{\Sigma}_2^{\frac{1}{2}}. \quad (3)$$

Then, the Fisher matrix is defined as

$$\mathbf{F} = \mathbf{S}_1 \mathbf{S}_2^{-1}, \quad (4)$$

which shares the same non-zero eigenvalues as the matrix

$$\mathbf{F} = \mathbf{R}_p^* \tilde{\mathbf{S}}_1 \mathbf{R}_p \tilde{\mathbf{S}}_2^{-1}. \quad (5)$$

Here, $\mathbf{R}_p = \mathbf{\Sigma}_1^{1/2} \mathbf{\Sigma}_2^{-1/2}$, $\tilde{\mathbf{S}}_1 = n_1^{-1} \mathbf{X} \mathbf{X}^*$ and $\tilde{\mathbf{S}}_2 = n_2^{-1} \mathbf{Y} \mathbf{Y}^*$ are the standardized sample covariance matrices. Thus, if there is no confusion, we denote the matrix in (5) as the Fisher matrix \mathbf{F} and study it from this point onward.

The eigenvalues of $\mathbf{R}_p^* \mathbf{R}_p = \mathbf{\Sigma}_2^{-1/2} \mathbf{\Sigma}_1 \mathbf{\Sigma}_2^{-1/2}$ are equivalent to those in the matrix $\mathbf{\Sigma}_1 \mathbf{\Sigma}_2^{-1}$. When the difference between $\mathbf{\Sigma}_1$ and $\mathbf{\Sigma}_2$ is general and does not adhere to the low-rank assumption, the spectrum of $\mathbf{R}_p^* \mathbf{R}_p$ aligns with the form specified in (2) and can be rewritten in descending order as

$$\beta_{p,1}, \beta_{p,2}, \dots, \beta_{p,p}.$$

Let $\beta_{p,j} = \alpha_k$, $j \in \mathcal{J}_k$, where \mathcal{J}_k denotes the set consisting of the ranks of the m_k -pole eigenvalue α_k . Then, $\alpha_1, \alpha_2, \dots, \alpha_K$ are the population spiked eigenvalues

with respective multiplicity $m_k, k = 1, 2, \dots, K$, satisfying $m_1 + m_2 + \dots + m_K = M$, where M is a fixed integer. The rest $\beta_{p,M+1}, \dots, \beta_{p,p}$ are non-spiked eigenvalues. Then, we call \mathbf{F} defined in (5) as the so-called generalized spiked Fisher matrix by assuming that these spikes are much larger than the remaining eigenvalues.

Throughout the paper, the empirical spectral distribution (ESD) of a $p \times p$ matrix \mathbf{A} , with eigenvalues denoted by $\{l_i(\mathbf{A})\}$, is defined as the probability measure $p^{-1} \sum_{i=1}^p \delta_{\{l_i(\mathbf{A})\}}$, where $\delta_{\{a\}}$ denotes the Dirac mass at a point a . For a given sequence of random matrices $\{\mathbf{A}_n\}$, the ESD of $\{\mathbf{A}_n\}$ converges, in a sense to be precise and when $n \rightarrow \infty$, to a limiting spectral distribution (LSD). To proceed further, we consider some regular assumptions in random matrix theory.

Assumption 2. Assuming that $c_{n_1} = p/n_1 \rightarrow c_1 \in (0, \infty)$ and $c_{n_2} = p/n_2 \rightarrow c_2 \in (0, 1)$ as $\min(p, n_1, n_2) \rightarrow \infty$.

Assumption 3. The matrix \mathbf{R}_p is a deterministic and non-negative definite Hermitian matrix, with all its eigenvalues bounded. Moreover, the ESD $H_n(t)$ of $\mathbf{R}_p^* \mathbf{R}_p$, generated by the population eigenvalues $\{\beta_{p,j}, j = 1, 2, \dots, p\}$, tends to a proper probability measure $H(t)$ as $\min(p, n_1, n_2) \rightarrow \infty$.

For the generalized spiked Fisher matrix in (5), let its sample eigenvalues be denoted as $l_1(\mathbf{F}) \geq l_2(\mathbf{F}) \geq \dots \geq l_p(\mathbf{F})$. To apply random matrix theory to hypothesis testing problems, we need to establish the central limit theory (CLT) of linear spectral statistics composed of these eigenvalues. To this end, we first focus on their first-order limits. Particularly, for the sample spiked eigenvalues $\{l_j(\mathbf{F}), j \in \mathcal{J}_k\}, k = 1, 2, \dots, K$ associated with the population spiked eigenvalue α_k , [11] obtained the following relationship under the separation condition $\min_{i \neq k} |\alpha_k/\alpha_i - 1| > d$ for some constant $d > 0$:

$$\frac{l_j(\mathbf{F})}{\psi_k} - 1 \rightarrow 0, a.s. \quad j \in \mathcal{J}_k, \quad (6)$$

where ψ_k is a function with respect to α_k , specifically expressed as

$$\psi_k := \psi(\alpha_k) = \frac{\alpha_k \left(1 - c_1 \int \frac{t}{t - \alpha_k} dH(t) \right)}{1 + c_2 \int \frac{\alpha_k}{t - \alpha_k} dH(t)}. \quad (7)$$

2.2. Test on the number of spikes: the general case

To test the number of spikes in a generalized spiked Fisher matrix, we focus on the following hypothesis

$$\mathcal{H}_0 : M = M_0 \quad \text{v.s.} \quad \mathcal{H}_1 : M \neq M_0, \quad (8)$$

where M_0 is the true number of spikes in $\mathbf{R}_p^* \mathbf{R}_p$.

Motivated by a classic likelihood ratio test statistic for testing the number of spikes in a one-sample spiked covariance matrix, we are going to propose a similar statistic for the generalized spiked Fisher matrix. More specifically, it is well-known that the likelihood ratio test statistic $-2 \log L$ is often used for the probability PCA model, where

$$L = \left(\frac{(\prod_{i=M+1}^p l_i)^{\frac{1}{p-M}}}{\sum_{i=M+1}^p l_i / (p-M)} \right)^{\frac{(p-M)n}{2}}.$$

It can be found that $-2 \log L$ primarily depends on $\sum_{i=M+1}^p l_i$ and $\sum_{i=M+1}^p \log(l_i)$. Inspired by this, for the hypothesis (8) in the generalized spiked Fisher matrix, we proposed the test statistic

$$\sum_{j=1}^p f\{l_j(\mathbf{F})\} - \sum_{j \in \mathcal{J}_k, k=1}^K f\{l_j(\mathbf{F})\}. \quad (9)$$

Here, $f \in \mathcal{A}$, and \mathcal{A} represents a set of analytic functions defined on an open set of the complex plane containing the supporting set of the LSD of the matrix \mathbf{F} . In statistical applications, the form of $f(x)$ varies from case to case, depending on the particular problem under consideration.

There has been some related work for the limit behavior of the sample eigenvalues of \mathbf{F} . For the linear spectral statistic $\sum_{j=1}^p f\{l_j(\mathbf{F})\}$, [28] developed its CLT applicable when the general Fisher matrix has no spikes, while [11] focused on the limit of sample spiked eigenvalues $l_j(\mathbf{F})$, $j \in \mathcal{J}_k$, $k = 1, 2, \dots, K$. However, neither [28] nor [11] can address the problem of testing the number of spikes individually. Therefore, we aim to establish the CLT of the partial linear spectral statistic in (9) under the null, offering a fresh perspective on this statistical problem.

To develop the asymptotic theory of the statistic in (9), we first introduce some intermediate notations. Let $F^{(c_1, c_2, H)}$ represent the LSD of the Fisher matrix \mathbf{F} , and $F^{(c_{n1}, c_{n2}, H_n)}$ be the counterpart of $F^{(c_1, c_2, H)}$ with the substitution of (c_1, c_2, H) with (c_{n1}, c_{n2}, H_n) . Moreover, we denote $m_{c_1, c_2}(z)$ as the Stieltjes transform of $F^{(c_1, c_2, H)}$, and $\underline{m}_{c_1, c_2}(z) = -(1 - c_1)z^{-1} + c_1 m_{c_1, c_2}(z)$. For brevity, the notation $\underline{m}_{c_1, c_2}(z)$ will be simplified to $\underline{m}(z)$. Additionally, let $\underline{m}_{c_2}(z)$ satisfy the equation $z = -\{\underline{m}_{c_2}(z)\}^{-1} + c_2 \int \{t + \underline{m}_{c_2}(z)\}^{-1} dH(t)$. We further define $h^2 = c_1 + c_2 - c_1 c_2$ and $m_0(z) = \underline{m}_{c_2}\{-\underline{m}(z)\}$. Then, the CLT of the statistic in (9) under the null hypothesis is established as follows, with its proof provided in Appendix A.

Theorem 2.1. *For the hypothesis testing problem (8), suppose that Assumptions 1 to 3 are satisfied. Then, under the null, the test statistic (9) follows*

$$T_{f, H} = \nu_{f, H}^{-\frac{1}{2}} \left\{ \sum_{j=1}^p f\{l_j(\mathbf{F})\} - \sum_{j \in \mathcal{J}_k, k=1}^K f\{l_j(\mathbf{F})\} - d_1(f, H_n) + d_2(f, \alpha, H) - \mu_{f, H} \right\} \\ \Rightarrow \mathcal{N}(0, 1), \quad (10)$$

where

$$\begin{aligned} d_1(f, H_n) &= p \int f(x) dF^{(c_{n1}, c_{n2}, H_n)}(x), \\ d_2(f, \alpha_k, H) &= \sum_{k=1}^K m_k f(\psi_k). \end{aligned} \quad (11)$$

The mean and variance terms, $\mu_{f,H}$ and $\nu_{f,H}$, are functions of m_0 and their expressions can be found in the equations (23) and (24).

In Theorem 2.1, a notable distinction from the CLT in [28] is the computation of the centering parameter $d_1(f, H_n)$ in (11), whose expression becomes more intricate for spiked Fisher matrices. When the function $f(x)$ involved in test statistics and the population ESD $H_n(t)$ have simple forms, explicit expressions for the center term can be computed, as demonstrated in the following section. However, when $f(x)$ and $H_n(t)$ become complex, the analytical expressions are not readily available. Similar to Remark 4.1 in [28], we propose a numerical procedure in the supplementary material to approximate $d_1(f, H_n)$ for generalized spiked Fisher matrices, thereby facilitating practical implementation and enhancing the applicability of our approach.

2.3. The low-rank case of $\Sigma_1 - \Sigma_2$

Recall the spiked Fisher matrix adhering to the formula (1), the difference Δ between Σ_1 and Σ_2 is of low rank. Thus, the spectrum of $\mathbf{R}_p^* \mathbf{R}_p$ is arranged in descending order as

$$\beta_{p,1}, \beta_{p,2}, \dots, \beta_{p,M}, 1 \dots, 1.$$

Here, $\beta_{p,j} = \alpha_k, j \in \mathcal{J}_k$, where $\alpha_1, \alpha_2, \dots, \alpha_K$ are spikes with multiplicity m_1, m_2, \dots, m_K , satisfying $m_1 + m_2 + \dots + m_K = M$. Within this framework, the LSD of $\mathbf{R}_p^* \mathbf{R}_p$ is $H(t) = \delta_{\{1\}}$. Therefore, the CLT in Theorem 2.1 can be rewritten as the following result, where the mean and variance terms take the form of contour integrals along the unit circle, as demonstrated in [27].

Corollary 2.1. *For the testing problem (8), suppose that Assumptions 1 to 3 and the condition $\Sigma_1 = \Sigma_2 + \Delta$ are satisfied, then the asymptotic distribution of the test statistic (9) can be expressed as*

$$T_{f,1} = \nu_{f,1}^{-\frac{1}{2}} \left\{ \sum_{j=1}^p f\{l_j(\mathbf{F})\} - \sum_{j \in \mathcal{J}_k, k=1}^K f\{l_j(\mathbf{F})\} - d_1(f, H_n) - \mu_{f,1} \right\} \Rightarrow \mathcal{N}(0, 1), \quad (12)$$

where

$$\begin{aligned}
d_1(f, H_n) &= p \int f(x) dF^{(c_{n1}, c_{n2}, H_n)}(x) - \sum_{k=1}^K m_k f\left(\frac{\alpha_k(1 - \alpha_k - c_1)}{1 - \alpha_k + c_2 \alpha_k}\right), \\
\mu_{f,1} &= \lim_{r \downarrow 1} \frac{q}{4\pi i} \oint_{|\xi|=1} f\left(\frac{1 + h^2 + 2h\Re(\xi)}{(1 - c_2)^2}\right) \left[\frac{1}{\xi - r^{-1}} + \frac{1}{\xi + r^{-1}} - \frac{2}{\xi + c_2/h} \right] d\xi \\
&\quad + \frac{\beta_x c_1 (1 - c_2)^2}{2\pi i h^2} \oint_{|\xi|=1} f\left(\frac{1 + h^2 + 2h\Re(\xi)}{(1 - c_2)^2}\right) \frac{1}{(\xi + c_2/h)^3} d\xi \\
&\quad + \frac{\beta_y (1 - c_2)}{4\pi i} \oint_{|\xi|=1} f\left(\frac{1 + h^2 + 2h\Re(\xi)}{(1 - c_2)^2}\right) \frac{\xi^2 - c_2/h^2}{(\xi + c_2/h)^2} \\
&\quad \cdot \left[\frac{1}{\xi - \sqrt{c_2}/h} + \frac{1}{\xi + \sqrt{c_2}/h} - \frac{2}{c_2/h} \right] d\xi,
\end{aligned}$$

and

$$\begin{aligned}
\nu_{f,1} &= - \lim_{r \downarrow 1} \frac{q+1}{4\pi^2} \oint_{|\xi_1|=1} \oint_{|\xi_2|=1} f\left(\frac{1 + h^2 + 2h\Re(\xi_1)}{(1 - c_2)^2}\right) f\left(\frac{1 + h^2 + 2h\Re(\xi_2)}{(1 - c_2)^2}\right) \\
&\quad \cdot \frac{1}{(\xi_1 - r\xi_2)^2} d\xi_1 d\xi_2 \\
&\quad - \frac{(\beta_x c_1 + \beta_y c_2)(1 - c_2)^2}{4\pi^2 h^2} \oint_{|\xi_1|=1} f\left(\frac{1 + h^2 + 2h\Re(\xi_1)}{(1 - c_2)^2}\right) \frac{1}{(\xi_1 + c_2/h)^2} d\xi_1 \\
&\quad \cdot \oint_{|\xi_2|=1} f\left(\frac{1 + h^2 + 2h\Re(\xi_2)}{(1 - c_2)^2}\right) \frac{1}{(\xi_2 + c_2/h)^2} d\xi_2.
\end{aligned}$$

Here, $\Re(z)$ represents the real part of z , $\beta_x = E|x_{11}|^4 - q - 2$ and $\beta_y = E|y_{11}|^4 - q - 2$ with $q = 1$ for real case and $q = 0$ for complex.

As mentioned in the likelihood ratio statistics $-2 \log L$, we select functions $f(x) = x$ and $f(x) = \log x$ as two examples to calculate more concise results for Corollary 2.1 when $H(t) = \delta_{\{1\}}$. The calculation details are presented in the supplementary material.

Example 1. If $f(x) = x$ and $H(t) = \delta_{\{1\}}$, the statistic in (10) simplifies to

$$T_{x,1} = \nu_{x,1}^{-\frac{1}{2}} \left\{ \sum_{j=1}^p l_j - \sum_{j \in \mathcal{J}_k, k=1}^K l_j - d_{x,1} - \mu_{x,1} \right\} \Rightarrow \mathcal{N}(0, 1),$$

where

$$\begin{aligned}
d_{x,1} &= \frac{p - M + \sum_{k=1}^K m_k \alpha_k}{1 - c_2} - \sum_{k=1}^K \frac{m_k \alpha_k (1 - \alpha_k - c_1)}{1 - \alpha_k + c_2 \alpha_k}, \\
\mu_{x,1} &= \frac{qc_2}{(1 - c_2)^2} + \frac{\beta_y c_2}{1 - c_2}, \quad \nu_{x,1} = \frac{(q+1)h^2}{(1 - c_2)^4} + \frac{\beta_x c_1 + \beta_y c_2}{(1 - c_2)^2}.
\end{aligned}$$

Example 2. If $f(x) = \log x$ and $H(t) = \delta_{\{1\}}$, the statistic in (10) simplifies to

$$T_{\log,1} = \nu_{\log,1}^{-\frac{1}{2}} \left\{ \sum_{j=1}^p \log(l_j) - \sum_{j \in \mathcal{J}_k, k=1}^K \log(l_j) - d_{\log,1} - \mu_{\log,1} \right\} \Rightarrow \mathcal{N}(0, 1),$$

where

$$d_{\log,1} = p \left\{ \frac{(1-c_2) \log(1-c_2)}{c_2} + \frac{(1-h^2) [\log(1-h^2) - \log(1-c_2)]}{c_2 - h^2} \right\} \\ - \sum_{k=1}^K m_k \log \left(\frac{1 - \alpha_k - c_1}{1 - \alpha_k + c_2 \alpha_k} \right),$$

$$\mu_{\log,1} = \frac{q}{2} \log \frac{1-h^2}{(1-c_2)^2} - \frac{\beta_x c_1 - \beta_y c_2}{2},$$

$$\nu_{\log,1} = -(q+1) \log(1-h^2) + (\beta_x c_1 + \beta_y c_2).$$

As presented in Corollary 2.1, the mean and variance terms in Examples 1 and 2 can be computed using the residues. When $f(x) = x$ and $f(x) = \log x$, some results relevant to computing contour integrals can be found in the references [8] and [27], which are utilized in the proofs of the above examples.

3. Application to large-dimensional linear regression models

In large-dimensional linear regression models, identifying the number of significant variables is crucial for helping measure the complexity of the model, which assists in further refining selection algorithms, such as LASSO or step-wise regression. This approach helps in focusing on truly influential predictors, which is useful in modern applications with large datasets.

In testing for significant variables, statistical tools like Wilk's likelihood ratio test (LRT) play an essential role. In large-dimensional settings, [4] developed a modified Wilk's test for the general linear hypothesis using random matrix theory, with the test statistic expressed as a function of eigenvalues of the standard Fisher matrix. However, their method cannot establish a direct relation with the number of significant variables and is thus unsuitable for tackling our current issue. To address it, we introduce a novel test statistic predicated on the eigenvalues of the spiked Fisher matrix, where the number of spikes in this matrix is equivalent to the number of significant variables. This approach offers a more targeted methodology for variable selection in high-dimensional data analysis.

Let the p -dimensional observations $\{\mathbf{z}_i\}_{1 \leq i \leq n}$ being from the following linear regression model:

$$\mathbf{z}_i = \mathbf{B}\mathbf{w}_i + \boldsymbol{\epsilon}_i, \quad i = 1, 2, \dots, n, \quad (13)$$

where $\{\mathbf{w}_i\}_{1 \leq i \leq n}$ are known design vectors (or regression variables) of dimension r , \mathbf{B} is a $p \times r$ matrix of regression coefficients, and $\{\epsilon_i\}_{1 \leq i \leq n}$ are a sequence of i.i.d. errors drawn from $\mathcal{N}_p(\mathbf{0}, \mathbf{V})$. We assume that $n \geq p + r$ and the rank of $\mathbf{W} = (\mathbf{w}_1, \mathbf{w}_2, \dots, \mathbf{w}_n)$ is r .

As a common manipulation, we partition the matrix \mathbf{B} as $(\mathbf{B}_1, \mathbf{B}_2)$, where \mathbf{B}_1 has r_1 columns and \mathbf{B}_2 has r_2 columns, satisfying $r_1 + r_2 = r$. To deal with large-dimensional data, we assume that $p/r_1 \rightarrow c_1 \in (0, \infty)$, $p/(n - r) \rightarrow c_2 \in (0, 1)$ as $\min(p, r_1, n - r) \rightarrow \infty$. Assuming that M_0 is the true number of non-zero columns of \mathbf{B}_1 , which is the true number of significant variables. Our goal is to test the hypothesis that:

$$\mathcal{H}_0 : M = M_0 \quad v.s. \quad \mathcal{H}_1 : M \neq M_0. \quad (14)$$

Divide \mathbf{w}_1^T into $(\mathbf{w}_{i,1}^T, \mathbf{w}_{i,2}^T)$ in a same manner corresponding to the partition of $\mathbf{B} = (\mathbf{B}_1, \mathbf{B}_2)$. Then, as elaborated in [4], the well-known Wilk's statistic can be written in terms of Wishart-distributed matrices as

$$\Lambda_n = \left| \mathbf{I} + \frac{r_1}{n - r} \mathbf{H}_0 \mathbf{G}^{-1} \right|^{-1}, \quad (15)$$

where $\mathbf{H}_0 = (\hat{\mathbf{B}}_1 - \mathbf{B}_1) \mathbf{A}_{11:2} (\hat{\mathbf{B}}_1 - \mathbf{B}_1)^T / r_1$, $\mathbf{G} = n \hat{\mathbf{V}} / (n - r)$. Here, $\mathbf{A}_{11:2} = \sum_{i=1}^n \mathbf{w}_{i,1} \mathbf{w}_{i,1}^T - \sum_{i=1}^n \mathbf{w}_{i,1} \mathbf{w}_{i,2}^T (\sum_{i=1}^n \mathbf{w}_{i,2} \mathbf{w}_{i,2}^T)^{-1} \sum_{i=1}^n \mathbf{w}_{i,2} \mathbf{w}_{i,1}^T$, and $\hat{\mathbf{B}}_1$ consists of the first r_1 columns of $\hat{\mathbf{B}}$ with $\hat{\mathbf{B}}$ being the maximum likelihood estimator of \mathbf{B} in the full parameter space. Under the null, by Lemmas 8.4.1 and 8.4.2 in [2], we can obtain that

$$(n - r) \mathbf{G} \sim W_p(\mathbf{V}, n - r), \quad r_1 \mathbf{H}_0 \sim W_p(\mathbf{V}, r_1), \quad (16)$$

and \mathbf{H}_0 is independent of \mathbf{G} , where $W_p(\cdot, \kappa)$ represents the p -dimensional Wishart distribution with κ degrees of freedom. Therefore, $\mathbf{H}_0 \mathbf{G}^{-1}$ is distributed as the Fisher matrix. According to [2], the logarithm-transformed LRT, $-\log \Lambda_n$, is traditionally employed as a test statistic for the general linear hypothesis.

To apply Theorem 2.1 to test the hypothesis (14), we first construct a spiked Fisher matrix with M_0 spikes. We start by decomposing \mathbf{H}_0 as $\mathbf{H}_0 = (\hat{\mathbf{B}}_1 \mathbf{A}_{11:2} \hat{\mathbf{B}}_1^T - \hat{\mathbf{B}}_1 \mathbf{A}_{11:2} \mathbf{B}_1^T - \mathbf{B}_1 \mathbf{A}_{11:2} \hat{\mathbf{B}}_1^T + \mathbf{B}_1 \mathbf{A}_{11:2} \mathbf{B}_1^T) / r_1$. Then define $\mathbf{H} = \hat{\mathbf{B}}_1 \mathbf{A}_{11:2} \hat{\mathbf{B}}_1^T / r_1$, so that

$$\mathbf{H} = \mathbf{H}_0 + \mathbf{\Delta}_0,$$

where $\mathbf{\Delta}_0 = (\hat{\mathbf{B}}_1 \mathbf{A}_{11:2} \mathbf{B}_1^T + \mathbf{B}_1 \mathbf{A}_{11:2} \hat{\mathbf{B}}_1^T - \mathbf{B}_1 \mathbf{A}_{11:2} \mathbf{B}_1^T) / r_1$. Here, $\mathbf{\Delta}_0$ has M_0 dominated eigenvalues, indicating the spikes, and thus the matrix \mathbf{H} represents a perturbation of rank M_0 on the matrix \mathbf{H}_0 . We demonstrate the spiked structure and the eigenvalue properties of \mathbf{H} in the supplementary material. Combining the formula (16), the matrix $\mathbf{H} \mathbf{G}^{-1}$ corresponds exactly to the spiked Fisher matrix with M_0 spikes defined in (4) under the null.

To test the number of significant regression variables, equivalent to testing the number of spikes, we use the perturbed matrix \mathbf{H} to design the modified

LRT statistic, given by

$$\Lambda_n^* = \left| \mathbf{I} + \frac{r_1}{n-r} \mathbf{H} \mathbf{G}^{-1} \right|^{-1}. \quad (17)$$

Denote the eigenvalues of $\mathbf{H} \mathbf{G}^{-1}$ in (17) in descending order as below:

$$l_1 \geq l_2 \geq \cdots \geq l_p,$$

where the largest M_0 eigenvalues are sample spiked eigenvalues. Then, the test statistic for the hypothesis (14) can be constructed as a partial linear spectral statistic defined in (9), with the function f using the traditional log transformation like [4], i.e.

$$-\log \Lambda_n^* - \sum_{i=1}^M \log\left(1 + \frac{c_2}{c_1} l_i\right).$$

Its CLT is established as follows, and the computation of mean and variance can be found in [4].

Theorem 3.1. *For the testing problem (14) in the large-dimensional linear regression model in (13), Λ_n^* is defined as in the formula (17), and it is assumed that $p/r_1 \rightarrow c_1 \in (0, \infty)$, $p/(n-r) \rightarrow c_2 \in (0, 1)$ as $\min(p, r_1, n-r) \rightarrow \infty$. Then, under the null, we have*

$$T_l = \nu_l^{-\frac{1}{2}} \left[-\log \Lambda_n^* - \sum_{i=1}^M \log\left(1 + \frac{c_2}{c_1} l_i\right) - d_{l1} + d_{l2} - \mu_l \right] \Rightarrow \mathcal{N}(0, 1), \quad (18)$$

where

$$d_{l1} = p \int \log\left(1 + \frac{c_2}{c_1} x\right) dF^{(c_{n1}, c_{n2}, H_n)}(x)$$

can be obtained by Algorithm 1 in the supplementary material,

$$d_{l2} = \sum_{i=1}^M \log\left(1 + \frac{c_2}{c_1} \psi_i\right), \mu_l = \frac{1}{2} \log \frac{(c^2 - d^2) h^2}{(ch - c_2 d)^2}, \text{ and } \nu_l = 2 \log \left(\frac{c^2}{c^2 - d^2} \right).$$

Here,

$$h = \sqrt{c_1 + c_2 - c_1 c_2}, \quad a, b = \frac{(1 \mp h)^2}{(1 - c_2)^2}, \quad a < b,$$

and

$$c, d = \frac{1}{2} \left(\sqrt{1 + \frac{c_2}{c_1} b} \pm \sqrt{1 + \frac{c_2}{c_1} a} \right), \quad c > d.$$

Based on Theorem 3.1, we can identify the number of significant variables through a sequential testing procedure. We initiate with $M_0 = 1$ and proceed with the sequential test until the statistic first falls within the acceptance domain. The number of significant variables is then determined by the position at which this occurs.

4. Application to change point detection

Change point detection can identify mutations of some statistical characteristics in sequence data. As a processing tool, it has proven useful in many applications such as DNA segmentation, econometrics, and disease demography. In this section, we will employ a hypothesis testing method to detect the change points. The test of the existence of change points will be transformed into testing whether there are spikes in the Fisher matrices constructed in the following way.

Given a p -dimensional sequence data $\mathbf{X} = (\mathbf{x}_1, \mathbf{x}_2 \cdots, \mathbf{x}_T)$ of length T with both change points and additive outliers, and the locations of which are unknown in practice. Additive outliers affect only a single or few specific observations, whereas change points occur over a relatively long period. Assuming that the change points occur at the time t_c , which needs to be correctly detected in practice while avoiding the influence of additive outliers.

As one of the fundamental tools, we use the point-by-point sliding time window for change point detection, which can be described below. At each step of sliding, the first sample in the window is removed, and a new sample is added at the end. Similar to [14], we partition the samples within each time window $W_j, j = 1, 2, \dots$ into two groups, with their respective population covariance matrices denoted as $\Sigma_j^{(1)}$ and $\Sigma_j^{(2)}$. Let the true number of spikes in the matrix $(\Sigma_j^{(1)})^{-1}\Sigma_j^{(2)}$ in the window W_j be denoted by $M_j, j = 1, 2, \dots$. When there are no anomalies in W_j , we have $(\Sigma_j^{(1)})^{-1}\Sigma_j^{(2)} = \mathbf{I}$, thus $M_j = 0$. Conversely, when anomalies are introduced in W_j , $M_j \neq 0$. To detect the change point in the time window W_j , we consider the following hypothesis

$$\mathcal{H}_0 : M_j = 0 \quad v.s. \quad \mathcal{H}_1 : M_j \neq 0, j = 1, 2, \dots \quad (19)$$

This is a degenerate hypothesis for the problem (8).

Denote $\mathbf{X}_j^{(1)}$ and $\mathbf{X}_j^{(2)}$ as the two distinct group of samples in the window W_j , with the sample size q_{j1} and q_{j2} , respectively. Then, the corresponding unbiased sample covariance matrices can be denoted by $\mathbf{S}_j^{(1)}$ and $\mathbf{S}_j^{(2)}$. Using the point-by-point sliding time window method, multiple tests are required, making the method inherently complex. To manage this complexity, a simple form of the test statistic, $\text{tr}[(\mathbf{S}_j^{(1)})^{-1}\mathbf{S}_j^{(2)}]$, is employed. The key observation is that the Fisher matrix $(\mathbf{S}_j^{(1)})^{-1}\mathbf{S}_j^{(2)}$ has no sample spikes under the null hypothesis, while it has spikes under the alternative hypothesis.

To develop the CLT of the test statistic, we introduce some notations. Normalize the first group of data $\mathbf{X}_j^{(1)}$ as $\boldsymbol{\xi}_j^{(1)}$, and the second group of data $\mathbf{X}_j^{(2)}$ as $\boldsymbol{\xi}_j^{(2)}$. Further, define $\phi_j^{(1)} = E \left| \xi_{j,11}^{(1)} \right|^4$, $\phi_j^{(2)} = E \left| \xi_{j,11}^{(2)} \right|^4$, where $\xi_{j,11}^{(1)}$ and $\xi_{j,11}^{(2)}$ are the (1,1)-th entries of the matrices $\boldsymbol{\xi}_j^{(1)}$ and $\boldsymbol{\xi}_j^{(2)}$, respectively. Then, the asymptotic distribution of the test statistic $\text{tr}[(\mathbf{S}_j^{(1)})^{-1}\mathbf{S}_j^{(2)}]$ is established as follows, which is a natural consequence of Theorem 2.1, and the calculation can refer to Example 1.

Corollary 4.1. *For the testing problem (19) in each window $W_j, j = 1, 2, \dots$, assuming that $p/q_{j1} \rightarrow c_j^{(1)} \in (0, 1)$, $p/q_{j2} \rightarrow c_j^{(2)} \in (0, +\infty)$ as $\min(p, q_{j1}, q_{j2}) \rightarrow \infty$. Then, under the null, we have*

$$T_j = \nu_x^{-\frac{1}{2}} \left\{ \text{tr}[(\mathbf{S}_j^{(1)})^{-1} \mathbf{S}_j^{(2)}] - d_x - \mu_x \right\} \Rightarrow \mathcal{N}(0, 1), \quad (20)$$

where

$$\begin{aligned} d_x &= \frac{p}{1 - c_j^{(1)}}, \\ \mu_x &= \frac{qc_j^{(1)}}{(1 - c_j^{(1)})^2} + \frac{\beta_j^{(1)}c_j^{(1)}}{1 - c_j^{(1)}}, \\ \nu_x &= \frac{(q+1)h_j^2}{(1 - c_j^{(1)})^4} + \frac{\beta_j^{(1)}c_j^{(1)} + \beta_j^{(2)}c_j^{(2)}}{(1 - c_j^{(1)})^2}. \end{aligned}$$

Here, $h_j^2 = (c_j^{(1)})^2 + (c_j^{(2)})^2 - c_j^{(1)}c_j^{(2)}$, $\beta_j^{(1)} = \phi_j^{(1)} - q - 2$ and $\beta_j^{(2)} = \phi_j^{(2)} - q - 2$ with $q = 1$ for real case and $q = 0$ for complex.

Based on Corollary 4.1, we design an algorithm to detect the location t_c of the change point, as elaborated in Algorithm 1. Note that the criterion for determining whether a change point is detected is that abnormal points are found in s consecutive windows.

Algorithm 1 Change Point Detection Based on Hypothesis Testing.

Input: $\mathbf{X} = (\mathbf{x}_1, \mathbf{x}_2, \dots, \mathbf{x}_T)$; q_{11}, q_{12} ; s ; an empty set \mathcal{T} .

Output: The location t_c of change point.

- 1: $j = 0$;
 - 2: **while** There are no s consecutive numbers in the set \mathcal{T} **do**
 - 3: $j = j + 1$;
 - 4: Partition the samples in the window W_j into two groups, and compute the respective sample covariance matrices as $\mathbf{S}_j^{(1)}$ and $\mathbf{S}_j^{(2)}$;
 - 5: Calculate T_j in the window W_j according to (20);
 - 6: **if** T_j falls outside the rejection region **then**
 - 7: Slide the Window to W_{j+1} ;
 - 8: **else**
 - 9: Delete the sample x_{t_0} at the end of W_j , where t_0 is the location of this sample in the data \mathbf{X} ;
 - 10: Add t_0 to the set \mathcal{T} ;
 - 11: Slide the Window to W_{j+1} ;
 - 12: **end if**
 - 13: **end while**
 - 14: Obtain the first value of the s consecutive numbers in \mathcal{T} as the location t_c where the change point occurs.
-

Remark 1. A critical step in Algorithm 1 is the removal of abnormal samples in step 9, which is essential for avoiding the influence of additive outliers on change point detection. Without this removal, the newly introduced additive outliers will exist in multiple consecutive time windows until they slip out

of the window, which can also produce consecutive s anomalous results and thus lead to false detection of change points. Furthermore, by the removal of abnormal points, for the lengths of two groups of data in all windows, we have $q_{11} = q_{21} = \dots = q_{j1} = \dots$ and $q_{12} \geq q_{22} \geq \dots \geq q_{j2} \geq \dots$.

5. Numerical and empirical studies

5.1. Evaluation for the CLT proposed in Theorem 2.1

To verify the effectiveness of our established CLT in Theorem 2.1, the following two models are considered.

Model 1: Assuming that the matrix $\mathbf{R}_p^* \mathbf{R}_p$ is non-diagonal, with $\mathbf{\Sigma}_2 = \mathbf{I}_p$ and $\mathbf{\Sigma}_1 = \mathbf{U} \text{diag}(10, 8, 8, 6, 1, \dots, 1) \mathbf{U}^*$, where \mathbf{U} is an orthogonal matrix.

Model 2: Assuming that the matrix $\mathbf{R}_p^* \mathbf{R}_p$ is diagonal, with $\mathbf{\Sigma}_2 = \mathbf{I}_p$ and $\mathbf{\Sigma}_1 = \text{diag}(36, 25, 25, 16, 2, \dots, 2, 1, \dots, 1)$. Here, “2” has multiplicity $p/2 - 4$, and “1” has multiplicity $p/2$.

In both models, the true number of spikes is $M_0 = 4$. Moreover, in Model 1, the LSD of $\mathbf{\Sigma}_1 \mathbf{\Sigma}_2^{-1}$ is $H(t) = \delta_{\{1\}}$, while in Model 2, the LSD is $H(t) = 0.5\delta_{\{1\}} + 0.5\delta_{\{2\}}$. In particular, the mean term $\mu_{f,H}$ and variance term $\nu_{f,H}$ in Model 2 can be obtained numerically by the procedure proposed in [28]. As a robustness check of our method, the samples $\{x_{ij}\}$ and $\{y_{il}\}$ in each model are generated from the following two populations.

Gaussian Assumption: Both $\{x_{ij}\}$ and $\{y_{il}\}$ are i.i.d. samples from $\mathcal{N}(0, 1)$.

Gamma Assumption: Both $\{x_{ij}\}$ and $\{y_{il}\}$ are i.i.d. samples from $\{\text{Gamma}(2, 1) - 2\} / \sqrt{2}$.

In such settings, four scenarios are considered. We select $f(x) = x$ and $f(x) = \log x$ as examples to conduct simulations. For each scenario, the value of dimensionality is set to $p = 100, 200, 400$. The ratio pairs (c_1, c_2) are set to $(0.8, 0.2), (2, 0.2), (0.2, 0.5)$ for $f(x) = x$, and $(0.5, 0.2), (0.4, 0.5), (0.2, 0.5)$ for $f(x) = \log x$, respectively.

Tables 1 and 2 report the empirical sizes and powers of rejecting the null hypothesis (8) over 1,000 replications in Models 1 and 2 at a significance level $\alpha = 0.05$ when $f(x) = \log(x)$. For space considerations, similar results for the function $f(x) = x$ are presented in the supplementary material. Under different models and population assumptions, the empirical sizes of our proposed test statistic are approximately equal to the significance level when the null hypothesis is true. The further the alternative hypothesis is from the null hypothesis, the higher the power is. From these results, it can be inferred that the true value M_0 aligns with the location of the first local minimum of empirical sizes. Furthermore, Figures 1 and 2 show the empirical density histograms of our proposed test statistic under the null for cases where $p = 200$. These figures suggest that the proposed statistic is asymptotically normal when the null hypothesis is true, further validating the effectiveness of our method.

TABLE 1
Empirical size of rejecting the null hypothesis (8) in Model 1 when $f(x) = \log x$.

Values of M_0	$M_0 = 1$	$M_0 = 2$	$M_0 = 3$	$M_0 = 4$	$M_0 = 5$	$M_0 = 6$
Gaussian population						
$p = 100, c_1 = 0.5, c_2 = 0.2$	0.993	0.785	0.251	0.050	0.083	0.154
$p = 200, c_1 = 0.5, c_2 = 0.2$	0.988	0.790	0.242	0.051	0.090	0.183
$p = 400, c_1 = 0.5, c_2 = 0.2$	0.992	0.803	0.265	0.054	0.079	0.188
$p = 100, c_1 = 0.4, c_2 = 0.5$	0.964	0.682	0.209	0.043	0.074	0.152
$p = 200, c_1 = 0.4, c_2 = 0.5$	0.97	0.658	0.198	0.047	0.090	0.253
$p = 400, c_1 = 0.4, c_2 = 0.5$	0.964	0.694	0.211	0.050	0.122	0.272
$p = 100, c_1 = 0.2, c_2 = 0.5$	0.990	0.774	0.263	0.053	0.106	0.204
$p = 200, c_1 = 0.2, c_2 = 0.5$	0.990	0.769	0.246	0.051	0.113	0.328
$p = 400, c_1 = 0.2, c_2 = 0.5$	0.989	0.800	0.260	0.052	0.134	0.352
Gamma population						
$p = 100, c_1 = 0.5, c_2 = 0.2$	0.863	0.482	0.132	0.045	0.060	0.084
$p = 200, c_1 = 0.5, c_2 = 0.2$	0.826	0.480	0.140	0.044	0.069	0.118
$p = 400, c_1 = 0.5, c_2 = 0.2$	0.845	0.471	0.139	0.045	0.070	0.133
$p = 100, c_1 = 0.4, c_2 = 0.5$	0.720	0.363	0.116	0.043	0.064	0.122
$p = 200, c_1 = 0.4, c_2 = 0.5$	0.755	0.397	0.137	0.051	0.075	0.149
$p = 400, c_1 = 0.4, c_2 = 0.5$	0.763	0.404	0.117	0.052	0.090	0.159
$p = 100, c_1 = 0.2, c_2 = 0.5$	0.836	0.456	0.146	0.042	0.068	0.121
$p = 200, c_1 = 0.2, c_2 = 0.5$	0.834	0.434	0.128	0.047	0.084	0.187
$p = 400, c_1 = 0.2, c_2 = 0.5$	0.854	0.464	0.159	0.052	0.096	0.190

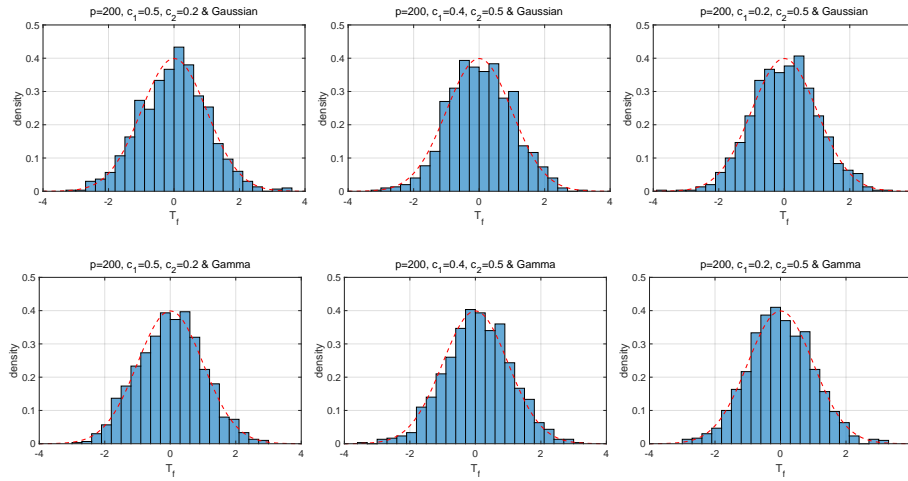


FIG 1. Empirical distribution of T_f under the null in Model 1 when $f(x) = \log x$.

TABLE 2
Empirical size of rejecting the null hypothesis (8) in Model 2 when $f(x) = \log x$.

Values of M_0	$M_0 = 1$	$M_0 = 2$	$M_0 = 3$	$M_0 = 4$	$M_0 = 5$	$M_0 = 6$
Gaussian population						
$p = 100, c_1 = 0.5, c_2 = 0.2$	0.999	0.900	0.290	0.045	0.374	0.915
$p = 200, c_1 = 0.5, c_2 = 0.2$	1	0.913	0.311	0.044	0.328	0.870
$p = 400, c_1 = 0.5, c_2 = 0.2$	1	0.938	0.359	0.045	0.282	0.872
$p = 100, c_1 = 0.4, c_2 = 0.5$	0.995	0.808	0.250	0.041	0.690	0.996
$p = 200, c_1 = 0.4, c_2 = 0.5$	0.999	0.858	0.308	0.051	0.617	0.999
$p = 400, c_1 = 0.4, c_2 = 0.5$	0.997	0.856	0.289	0.050	0.678	0.995
$p = 100, c_1 = 0.2, c_2 = 0.5$	0.999	0.888	0.294	0.052	0.693	0.997
$p = 200, c_1 = 0.2, c_2 = 0.5$	0.999	0.918	0.334	0.052	0.627	0.996
$p = 400, c_1 = 0.2, c_2 = 0.5$	1	0.917	0.324	0.056	0.825	1
Gamma population						
$p = 100, c_1 = 0.5, c_2 = 0.2$	0.929	0.577	0.157	0.040	0.213	0.616
$p = 200, c_1 = 0.5, c_2 = 0.2$	0.955	0.649	0.200	0.048	0.223	0.654
$p = 400, c_1 = 0.5, c_2 = 0.2$	0.949	0.629	0.191	0.053	0.220	0.661
$p = 100, c_1 = 0.4, c_2 = 0.5$	0.892	0.507	0.147	0.045	0.352	0.897
$p = 200, c_1 = 0.4, c_2 = 0.5$	0.880	0.516	0.153	0.047	0.257	0.810
$p = 400, c_1 = 0.4, c_2 = 0.5$	0.878	0.491	0.146	0.054	0.244	0.824
$p = 100, c_1 = 0.2, c_2 = 0.5$	0.938	0.615	0.182	0.043	0.466	0.954
$p = 200, c_1 = 0.2, c_2 = 0.5$	0.958	0.606	0.183	0.046	0.492	0.955
$p = 400, c_1 = 0.2, c_2 = 0.5$	0.961	0.662	0.213	0.049	0.376	0.944

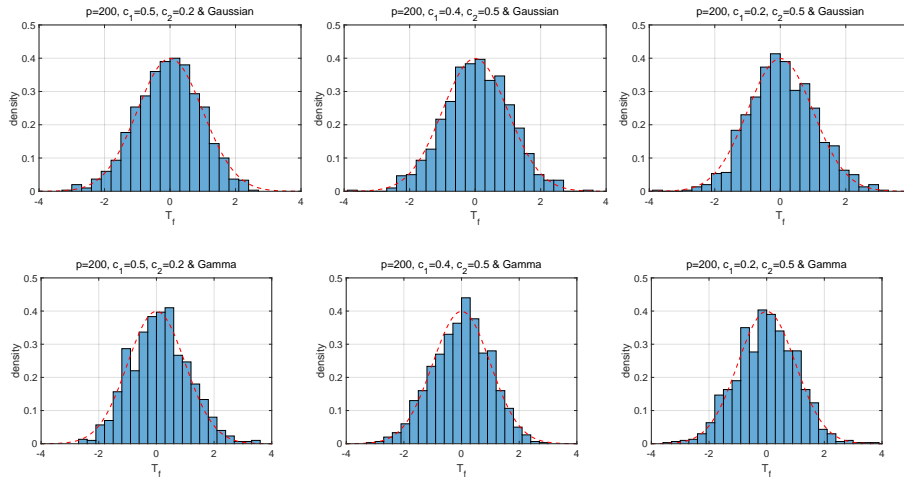


FIG 2. Empirical distribution of T_f under the null in Model 2 when $f(x) = \log x$.

5.2. Numerical studies for large-dimensional linear regression

For the hypothesis (14) in the large-dimensional linear regression model, we generate data from the following form:

$$\mathbf{z}_i = \mathbf{B}\mathbf{w}_i + \boldsymbol{\epsilon}_i, \quad i = 1, 2, \dots, n,$$

where the entries of regression variables \mathbf{w}_i are i.i.d. drawn from $\mathcal{N}(0, 1)$, the regression coefficient matrix \mathbf{B} is decomposed into $(\mathbf{B}_1, \mathbf{B}_2)$, $\mathbf{B}_1 = (\mathbf{b}_1, \mathbf{b}_2, \mathbf{b}_3, \mathbf{b}_4, \mathbf{b}_5, \mathbf{0}, \mathbf{0}, \dots, \mathbf{0})$ with the entries of $\mathbf{b}_i (i = 1, 2, \dots, 5)$ being i.i.d. from $\mathcal{N}(0, 1)$, and $\mathbf{B}_2 = \mathbf{0}$. Thus, $M_0 = 5$. The error $\boldsymbol{\epsilon}_i$ is a $p \times 1$ random vector drawn from $\mathcal{N}_p(\mathbf{0}, \mathbf{V})$, where the population covariance matrix \mathbf{V} is designed as the following two models.

Model 3: Assuming that the matrix \mathbf{V} is an identity matrix.

Model 4: Assuming that the matrix \mathbf{V} is in the form of a Toeplitz matrix defined as

$$\mathbf{V} = \begin{pmatrix} 1 & \rho & \rho^2 & \dots & \rho^{p-1} \\ \rho & 1 & \rho & \dots & \rho^{p-2} \\ \dots & \dots & \dots & \dots & \dots \\ \rho^{p-1} & \rho^{p-2} & \dots & \rho & 1 \end{pmatrix},$$

where $\rho = 0.9$.

In each scenario, the value of c_1 is set to 0.5, 1.5, and c_2 is set to 0.2, 0.5, 0.8. Reported in Tables 3 and 4 are the empirical sizes and powers of our proposed test statistic T_l in (3.1) rejecting the null with 2,000 replications at a significance level $\alpha = 0.05$, for Models 3 and 4, respectively.

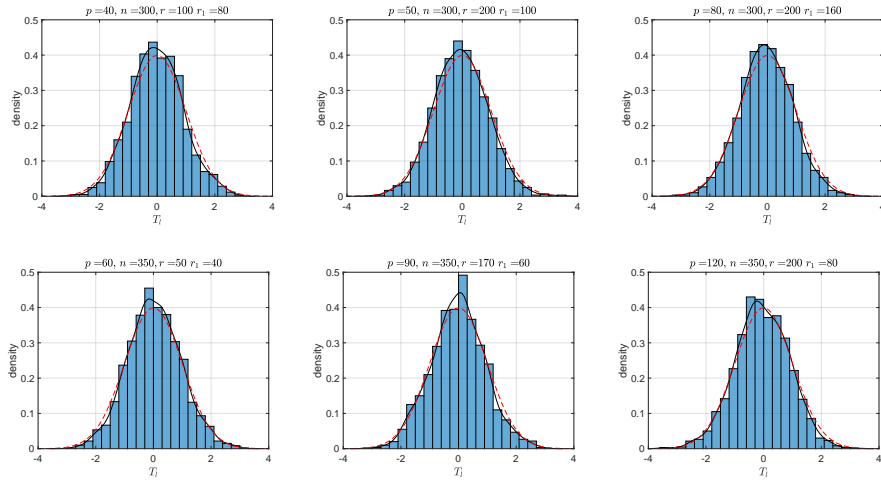


FIG 3. Empirical distribution of T_l under the null in Model 3.

As shown in the tables, the empirical sizes of our proposed test can consistently achieve correct empirical sizes around 0.05 for all models. Moreover, as the

TABLE 3
Empirical size of rejecting the null in Model 3.

	$M_0 = 1$	$M_0 = 2$	$M_0 = 3$	$M_0 = 4$	$M_0 = 5$	$M_0 = 6$
$p = 40, n = 300, r = 100, r_1 = 80$	1	1	1	1	0.0365	0.7450
$p = 80, n = 600, r = 200, r_1 = 160$	1	1	1	1	0.0395	0.7895
$p = 160, n = 1200, r = 400, r_1 = 320$	1	1	1	1	0.0515	0.8125
$p = 50, n = 300, r = 200, r_1 = 100$	1	1	1	0.9995	0.0360	0.7710
$p = 100, n = 600, r = 400, r_1 = 200$	1	1	1	1	0.0430	0.8055
$p = 200, n = 1200, r = 800, r_1 = 400$	1	1	1	1	0.0515	0.8305
$p = 80, n = 300, r = 200, r_1 = 160$	1	1	1	0.9790	0.0365	0.8245
$p = 160, n = 600, r = 400, r_1 = 320$	1	1	1	0.9955	0.0405	0.8580
$p = 320, n = 1200, r = 800, r_1 = 640$	1	1	1	0.9995	0.0480	0.8360
$p = 60, n = 350, r = 50, r_1 = 40$	1	1	1	1	0.0390	0.6830
$p = 120, n = 700, r = 100, r_1 = 80$	1	1	1	1	0.0395	0.7700
$p = 240, n = 1400, r = 200, r_1 = 160$	1	1	1	1	0.0460	0.7650
$p = 90, n = 350, r = 170, r_1 = 60$	1	1	1	1	0.0370	0.7555
$p = 180, n = 700, r = 340, r_1 = 120$	1	1	1	1	0.0420	0.7810
$p = 360, n = 1400, r = 680, r_1 = 240$	1	1	1	1	0.0480	0.7850
$p = 120, n = 350, r = 200, r_1 = 80$	1	1	1	1	0.0375	0.7965
$p = 240, n = 700, r = 400, r_1 = 160$	1	1	1	1	0.0420	0.8250
$p = 480, n = 1400, r = 800, r_1 = 320$	1	1	1	1	0.0515	0.8300

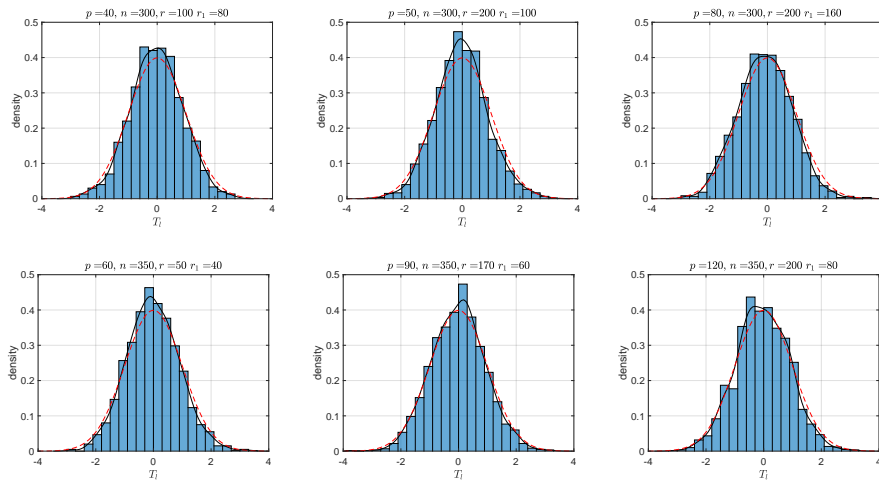


FIG 4. Empirical distribution of T_i under the null in Model 4.

TABLE 4
Empirical size of rejecting the null in Model 4.

Values of M_0	$M_0 = 1$	$M_0 = 2$	$M_0 = 3$	$M_0 = 4$	$M_0 = 5$	$M_0 = 6$
$p = 40, n = 300, r = 100, r_1 = 80$	1	1	1	1	0.0340	0.7410
$p = 80, n = 600, r = 200, r_1 = 160$	1	1	1	1	0.0440	0.7890
$p = 160, n = 1200, r = 400, r_1 = 320$	1	1	1	1	0.0465	0.7925
$p = 50, n = 300, r = 200, r_1 = 100$	1	1	1	1	0.0380	0.7890
$p = 100, n = 600, r = 400, r_1 = 200$	1	1	1	1	0.0425	0.8040
$p = 200, n = 1200, r = 800, r_1 = 400$	1	1	1	1	0.0550	0.814
$p = 80, n = 300, r = 200, r_1 = 160$	1	1	1	0.9995	0.0360	0.8315
$p = 160, n = 600, r = 400, r_1 = 320$	1	1	1	1	0.0415	0.8515
$p = 320, n = 1200, r = 800, r_1 = 640$	1	1	1	1	0.0520	0.8500
$p = 60, n = 350, r = 50, r_1 = 40$	1	1	1	1	0.0350	0.7040
$p = 120, n = 700, r = 100, r_1 = 80$	1	1	1	1	0.0440	0.7525
$p = 240, n = 1400, r = 200, r_1 = 160$	1	1	1	1	0.0450	0.7825
$p = 90, n = 350, r = 170, r_1 = 60$	1	1	1	1	0.0345	0.7525
$p = 180, n = 700, r = 340, r_1 = 120$	1	1	1	1	0.0345	0.7770
$p = 360, n = 1400, r = 680, r_1 = 240$	1	1	1	1	0.0475	0.7920
$p = 120, n = 350, r = 200, r_1 = 80$	1	1	1	1	0.0340	0.7980
$p = 240, n = 700, r = 400, r_1 = 160$	1	1	1	1	0.0410	0.8130
$p = 480, n = 1400, r = 800, r_1 = 320$	1	1	1	1	0.0445	0.8355

distance between the alternative and null hypotheses increases, so does the power of the test. Figures 3 and 4 depict the simulated empirical distributions of our proposed test statistic when the null hypothesis is true in several cases in Models 3 and 4. We can find that the empirical distribution of the statistic fits well with the standard normal distribution. Moreover, note that the parameter ρ defined in Model 4 represents the degree of correlation among the p components of error vectors, where $\rho = 0$ corresponds to the case of Model 3. Models 3 and 4 represent scenarios where the errors are completely uncorrelated or strongly correlated. The results indicate that our test method can provide good sizes irrespective of the correlations among the coordinates of the error vectors. In summary, our proposed test method can accurately determine the number of significant variables in different scenarios.

5.3. Numerical studies for change point detection

For the change point detection problem, we conduct simulations to compare our proposed method with three other methods from the existing literature, which are referred to as M-P, MSR, and SVM, described as follows.

- (a). **M-P:** [22] finds the change point by judging whether the largest eigenvalue of the sample covariance matrix falls outside the support set of the standard Marčenko-Pastur law.

- (b). **MSR:** [26] detects the change point by judging whether the mean spectral radius (MSR) calculated from the sample data is smaller than the inner ring radius of the single ring law.
- (c). **SVM:** With the classifications of normal data and abnormal data, [12] use training data to obtain Support Vector Machines (SVM) model, and predict whether there is an abnormality in the test data.

Similar to our change point detection method, when anomalies are detected in s consecutive windows using these three methods, it is considered that a change point has been detected.

For the data generation, we consider the following two models.

Model 5: $\mathbf{x}_t \stackrel{\text{i.i.d.}}{\sim} \mathcal{N}_p(\boldsymbol{\mu}, \mathbf{I}_p)$ for $1 \leq t \leq \lfloor 2T/3 \rfloor$, $\mathbf{x}_t \stackrel{\text{i.i.d.}}{\sim} \mathcal{N}_p(\boldsymbol{\mu}, \rho_1 \mathbf{I}_p)$ for $\lfloor 2T/3 \rfloor + 1 \leq t \leq T$, where $\boldsymbol{\mu} = (0.6, 0.6, \dots, 0.6) \in \mathbb{R}^p$.

Model 6: $\mathbf{x}_t = \mathbf{A}\mathbf{F}_t + \mathbf{e}_t$, where \mathbf{A} is a $p \times 5$ factor loading matrix with each element generated from a uniform distribution $U(0.5, 1.5)$, the factors $\mathbf{F}_t \stackrel{\text{i.i.d.}}{\sim} \mathcal{N}_5(\mathbf{0}, \mathbf{I}_5)$ and the error terms $\mathbf{e}_t \stackrel{\text{i.i.d.}}{\sim} \mathcal{N}_p(\mathbf{0}, \boldsymbol{\Sigma}_e)$. Here, $\boldsymbol{\Sigma}_e = \mathbf{I}_p$ for $1 \leq t \leq \lfloor 2T/3 \rfloor$, and $\boldsymbol{\Sigma}_e = (\sigma_{ij})_{i,j=1}^p$ with $\sigma_{ij} = \rho_2 0.8^{|i-j|}$ for $\lfloor 2T/3 \rfloor + 1 \leq t \leq T$.

In both models, the generated data have a length of $T = 6000$. Within these 6000 observations, two additive outliers are introduced at $t = 2001$ and $t = 2002$, with values of $20(\mathbf{1}_p, \mathbf{1}_p)$. Moreover, each model involves a parameter, ρ_1 or ρ_2 , which can reflect the magnitude of the distributional change. For instance, in Model 5, the larger the ρ_1 , the larger the difference between the covariance matrices before and after the time $2T/3$. We set $\rho_1 = 5, 10, 20$ in Model 5, and $\rho_2 = 3, 6, 9$ in Model 6, respectively. For each scenario, 100 pieces of simulated data are generated, with $s = 20$, and $q_{11} = q_{12} = 2p$. Accuracy, defined as the percentage of correctly detected change points, is used to evaluate the detection performance. Furthermore, note that our change point detection method requires multiple tests, increasing the risk of false positives. While the Bonferroni correction ([5]) is commonly used to adjust for this, it is too conservative. Instead, we empirically tested six significance levels ($\alpha = 0.0001, 0.0005, 0.001, 0.005, 0.01, 0.05$) to find the one that yields around 95% accuracy. Based on absolute error comparisons, we found that $\alpha = 0.0005$ minimizes error and is thus selected for further simulations. More details about the selection of α can be found in the supplementary material.

We set the dimension p to 50 and 100 for each model and compute the accuracy values, which are reported in Figure 5. Overall, it is evident that our proposed method outperforms the other three. Across various scenarios, the detection accuracy of our proposed test method reaches as high as about 95%. In contrast, the M-P method consistently demonstrates the lowest detection accuracy among both models. The MSR method exhibits strong performance only when the fluctuation of the change is substantial but fails when the fluctuation is minimal, such as in cases where $\rho_1 = 5$ and $\rho_1 = 10$ in Model 5. Furthermore, for the factor model setting in Model 6, both the M-P method and the MSR method fail, indicating that these methods are unsuitable for data with spiked structures. Whereas our method achieves high detection accuracy in all cases across different models. Additionally, the SVM method performs well in Model 5, achieving high

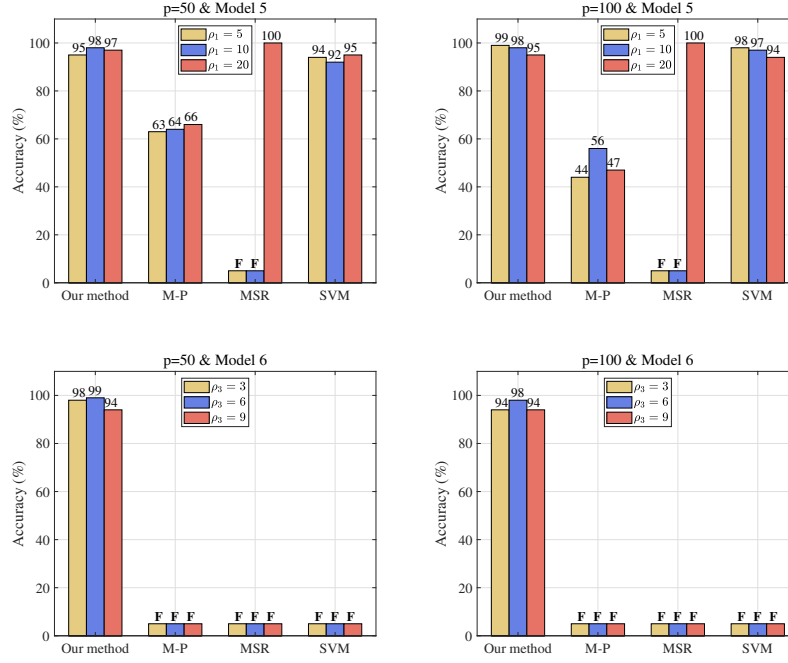


FIG 5. Accuracy comparisons among different methods in Models 5 and 6. The mark **F** indicates that the method fails.

accuracy. However, for Model 6 where the covariance matrix of the data exhibits a complex spiked structure, the SVM method also fails. Our method, on the other hand, continues to demonstrate high accuracy, indicating its robustness and suitability for data with complex structures.

5.4. Empirical study

In this section, we evaluate the performance of our proposed change point detection method through an empirical analysis of a monthly database for macroeconomic research (FRED-MD, [17]), which is available from the website <https://research.stlouisfed.org/econ/mccracken/fred-databases/>. The FRED-MD dataset comprises monthly series data for 128 macroeconomic variables spanning from January 1959 to June 2024. To ensure the data's suitability for analysis, we conduct several pre-processing steps: removing missing data, transforming the remaining data into a stationary form, and standardizing variables. Following the pre-processing, the data dimension and sample size are adjusted to $p = 103$ and $n = 783$, respectively.

In Figure 6, we plot the changes of the 103 features in the original data over time. Notably, around 2008, several indicators experienced significant fluctuations,

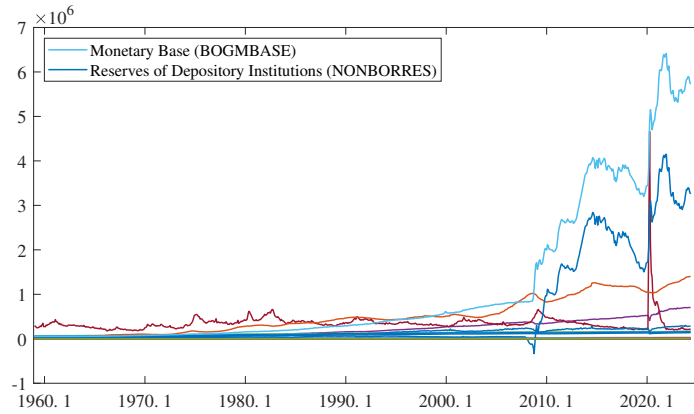


FIG 6. The monthly database for macroeconomic research (FRED-MD).

suggesting the occurrence of a change point during this period. The two most volatile indicators are the Reserves of Depository Institutions (NONBORRES) and the Monetary Base (BOGMBASE), reflecting some of the policy responses to the 2008 global financial crisis.

Due to the complex structure of the actual data and the challenge in satisfying the column independence condition, the asymptotic distribution of the test statistic T_j deviates to some extent from Corollary 4.1. To address this, we refer to [14] and use the upper 95% quantile of the empirical distributions of $T_j, j = 1, 2, \dots$ to adjust the original threshold of the rejection region. For parameter settings, we chose $q_{11} = p + 50$ and $q_{12} = p - 10$, with s set to 10. Change point detection was performed using Algorithm 1, and the results identified the change point at the 595th time point, corresponding to July 2008. This finding aligns with our analysis in Figure 6, validating the effectiveness of the proposed methods on real-world data.

6. Conclusion

This paper discussed the problems of testing the number of spikes in a generalized spiked Fisher matrix. We proposed a universal test for this hypothesis testing problem, considered the partial linear spectra statistic as the test statistic, and established its CLT under the null hypothesis. The theoretical results of our test method were applied to two problems, large-dimensional linear regression and change point detection. The exceptional effectiveness and generality of our proposed methods were demonstrated through extensive numerical and empirical studies. Being independent of the population distribution and diagonal assumption of the population covariance matrix, our approaches have superior performance. Furthermore, the problem of testing the spikes in a non-central spiked Fisher matrix is also important and thus warrants further research.

Appendix A: Proof of Theorem 2.1

Proof. We need to prove the CLT of the following partial linear spectral statistic

$$T = \sum_{j=1}^p f\{l_j(\mathbf{F})\} - \sum_{j \in \mathcal{J}_k, k=1}^K f\{l_j(\mathbf{F})\}. \quad (21)$$

We first focus on the calculation of the second term $\sum_{j \in \mathcal{J}_k, k=1}^K f\{l_j(\mathbf{F})\}$ in (21). It is known that, for the sample spiked eigenvalues of \mathbf{F} , almost surely,

$$\sum_{j \in \mathcal{J}_k, k=1}^K f\{l_j(\mathbf{F})\} \rightarrow \sum_{k=1}^K m_k f(\psi_k), \quad (22)$$

where ψ_k is defined in (7).

For the first term in (21), we have

$$\begin{aligned} \sum_{j=1}^p f\{l_j(\mathbf{F})\} &= p \int f(x) dF_{\mathbf{n}}(x) \\ &= p \int f(x) d \left[F_{\mathbf{n}}(x) - F^{(c_{n1}, c_{n2}, H_n)}(x) \right] + p \int f(x) dF^{(c_{n1}, c_{n2}, H_n)}(x), \end{aligned}$$

where $F_{\mathbf{n}}$ is the ESD of the Fisher matrix \mathbf{F} , and $F^{(c_{n1}, c_{n2}, H_n)}$ is the distribution function in which the parameter (c_1, c_2, H) is replaced by (c_{n1}, c_{n2}, H_n) in the LSD of \mathbf{F} .

We consider the following centered and scaled variables

$$p \int f(x) d \left[F_{\mathbf{n}}(x) - F^{(c_{n1}, c_{n2}, H_n)}(x) \right] =: G_n(x).$$

Therefore, we have

$$G_n(x) = \sum_{j=1}^p f\{l_j(\mathbf{F})\} - p \int f(x) dF^{(c_{n1}, c_{n2}, H_n)}(x).$$

Under different population assumptions, both of [27] and [28] proved that the process $G_n(x)$ would converge weakly to a Gaussian vector with explicit expressions of means and covariance functions when the dimensions are proportionally large compared to the sample sizes. The arrays of two random vectors in the Fisher matrix considered by [27] can be independent but differently distributed. [28] further explored general Fisher matrices with arbitrary population covariance matrices, their proposed CLT extended and covered the conclusion of [27], and can be expressed as follows

$$G_n(x) \Rightarrow \mathcal{N}(\mu_{f,H}, \nu_{f,H}),$$

where

$$\begin{aligned}
\mu_{f,H} &= \frac{q}{4\pi i} \oint f(z) d \log \left[\frac{h^2}{c_2} - \frac{c_1}{c_2} \frac{\left\{ 1 - c_2 \int \frac{m_0(z)}{t+m_0(z)} dH(t) \right\}^2}{1 - c_2 \int \frac{m_0^2(z)}{\{t+m_0(z)\}^2} dH(t)} \right] \\
&+ \frac{q}{4\pi i} \oint f(z) d \log \left[1 - c_2 \int \frac{m_0^2(z) dH(t)}{\{t+m_0(z)\}^2} \right] \\
&- \frac{\beta_x c_1}{2\pi i} \oint f(z) \frac{z^2 \underline{m}^3(z) h_{m_1}(z)}{\frac{h^2}{c_2} - \frac{c_1}{c_2} \frac{\left\{ 1 - c_2 \int \frac{m_0(z)}{t+m_0(z)} dH(t) \right\}^2}{1 - c_2 \int \frac{m_0^2(z)}{\{t+m_0(z)\}^2} dH(t)}} dz \\
&+ \frac{\beta_y c_2}{2\pi i} \oint f(z) \underline{m}'(z) \frac{m^3(z) m_0^3(z) h_{m_2} \{-\underline{m}^{-1}(z)\}}{1 - c_2 \int \frac{m_0^2(z)}{\{t+m_0(z)\}^2} dH(t)} dz, \tag{23}
\end{aligned}$$

$$\begin{aligned}
\nu_{f,H} &= -\frac{q+1}{4\pi^2} \oint \oint \frac{f(z_1) f(z_2)}{\{m_0(z_1) - m_0(z_2)\}^2} dm_0(z_1) dm_0(z_2) \\
&- \frac{\beta_x c_1}{4\pi^2} \oint \oint f(z_1) f(z_2) \frac{\partial^2 [z_1 z_2 \underline{m}(z_1) \underline{m}(z_2) h_{v_1}(z_1, z_2)]}{\partial z_1 \partial z_2} dz_1 dz_2 \\
&- \frac{\beta_y c_2}{4\pi^2} \oint \oint f(z_1) f(z_2) \frac{\partial^2 [\underline{m}(z_1) m_0(z_1) \underline{m}(z_2) m_0(z_2) h_{v_2}(-\underline{m}^{-1}(z_1), -\underline{m}^{-1}(z_2))]}{\partial z_1 \partial z_2} dz_1 dz_2. \tag{24}
\end{aligned}$$

Here, $\beta_x = \mathbb{E}|x_{11}|^4 - q - 2$ and $\beta_y = \mathbb{E}|y_{11}|^4 - q - 2$ with $q = 1$ for real case and 0 for complex,

$$\begin{aligned}
h_{m_1}(z) &= -\frac{\frac{m_0^2(z)}{z^2 \underline{m}(z)} \int \frac{t^2}{(t+m_0(z))^3} dH(t)}{1 - c_2 \int \frac{m_0^2(z)}{(t+m_0(z))^2} dH(t)}, \\
h_{m_2}(-\underline{m}^{-1}(z)) &= -\frac{1}{\underline{m}^3(z)} \int \frac{t}{(t+m_0(z))^3} dH(t), \\
h_{v_1}(z_1, z_2) &= \frac{1}{z_1 z_2 \underline{m}(z_1) \underline{m}(z_2)} \int \frac{t^2}{(t+m_0(z_1))(t+m_0(z_2))} dH(t), \\
h_{v_2}(-\underline{m}^{-1}(z_1), -\underline{m}^{-1}(z_2)) &= \frac{1}{\underline{m}(z_1) \underline{m}(z_2)} \int \frac{1}{(t+m_0(z_1))(t+m_0(z_2))} dH(t).
\end{aligned}$$

The contours all contain the support of the LSD of \mathbf{F} and are non-overlapping in (23) and (24).

Then

$$G_n(x) - \sum_{j \in \mathcal{J}_k, k=1}^K f\{l_j(\mathbf{F})\} + \sum_{k=1}^K m_k f(\psi_k) \Rightarrow \mathcal{N}(\mu_{f,H}, \nu_{f,H}),$$

which is equivalent to

$$\nu_{f,H}^{-\frac{1}{2}} \left\{ G_n(x) - \sum_{j \in \mathcal{J}_k, k=1}^K f\{l_j(\mathbf{F})\} + \sum_{k=1}^K m_k f(\psi_k) - \mu_{f,H} \right\} \Rightarrow \mathcal{N}(0, 1).$$

Proof is completed. \square

Acknowledgments

The authors would like to thank the anonymous referees, the Associate Editors, and the Editor for their constructive comments of this paper.

Funding

The second author was supported by Key technologies for coordination and interoperation of power distribution service resource Grant No. 2021YFB2401300, and National Natural Science Foundation of China Grant No. 12326606.

Supplementary Material

Supplementary materials contain an algorithm to approximate the center parameter term $d_1(f, H_n)$ in Theorem 2.1, calculation details of Examples 1 and 2, an illustration about properties of the matrix \mathbf{H} in Section 3, the additional simulation results for Section 5.1, and details of the selection method of the significance level α in Section 5.3.

References

- [1] ALESSI, L., BARIGOZZI, M. and CAPASSO, M. (2010). Improved penalization for determining the number of factors in approximate factor models. *Statistics & Probability Letters* **80** 1806-1813.
- [2] ANDERSON, T. W. (2003). *An Introduction to Multivariate Statistical Analysis*. John Wiley & Sons.
- [3] BAI, J. and NG, S. (2002). Determining the Number of Factors in Approximate Factor Models. *Econometrica* **70** 191-221.
- [4] BAI, Z., JIANG, D., YAO, J. and RONG ZHENG, S. (2013). Testing linear hypotheses in high-dimensional regressions. *Statistics* **47** 1207 - 1223.
- [5] BONFERRONI, C. E. (1936). *Teoria statistica delle classi e calcolo delle probabilità. Pubblicazioni del R. Istituto superiore di scienze economiche e commerciali di Firenze*. Seeber.
- [6] DANDAN JIANG, Z. B. ZHIQIANG HOU and LI, R. (2023). Invariance Principle and CLT for the Spiked Eigenvalues of Large-dimensional Fisher Matrices and Applications. *Statistica Sinica*. Preprint.

- [7] HASTIE, T. J., BUJA, A. and TIBSHIRANI, R. (1995). Penalized Discriminant Analysis. *Annals of Statistics* **23** 73-102.
- [8] JIANG, D. (2017). Likelihood-based tests on moderate-high-dimensional mean vectors with unequal covariance matrices. *Journal of The Korean Statistical Society* **46** 451-461.
- [9] JIANG, D. (2023). A universal test on spikes in a high-dimensional generalized spiked model and its applications. *Statistica Sinica* **33** 1749-1770.
- [10] JIANG, D., HAO, H., YANG, L. and WANG, R. (2022). TOSE: A Fast Capacity Estimation Algorithm Based on Spike Approximations. *2022 IEEE 96th Vehicular Technology Conference (VTC2022-Fall)*.
- [11] JIANG, D., HOU, Z. and HU, J. (2021). The limits of the sample spiked eigenvalues for a high-dimensional generalized Fisher matrix and its applications. *Journal of Statistical Planning and Inference* **215** 208-217.
- [12] JIXIU, HONGYAN, Z., YUE, J., XUTING, Y. and HUI, W. (2015). Based on SVM power quality disturbance classification algorithm. In *The 27th Chinese Control and Decision Conference (2015 CCDC)* 3618-3621.
- [13] JOHNSTONE, I. M. (2001). On the distribution of the largest eigenvalue in principal components analysis. *The Annals of Statistics* **29** 295 – 327.
- [14] KE CHEN, B. W. DANDAN JIANG and WANG, H. (2022). Fisher Matrix Based Fault Detection for PMUs Data in Power Grids. arXiv:2208.04637.
- [15] KRITCHMAN, S. and NADLER, B. (2008). Determining the number of components in a factor model from limited noisy data. *Chemometrics and Intelligent Laboratory Systems* **94** 19-32.
- [16] MARIO FORNI, M. L. DOMENICO GIANNONE and REICHLIN, L. (2009). Opening the Black Box: Structural Factor Models with Large Cross Sections. *Econometric Theory* **25** 1319-1347.
- [17] MCCRACKEN, M. W. and NG, S. (2016). FRED-MD: A monthly database for macroeconomic research. *Journal of Business & Economic Statistics* **34** 574–589.
- [18] PASSEMIER, D., LI, Z. and YAO, J. (2017). On estimation of the noise variance in high dimensional probabilistic principal component analysis. *Journal of the Royal Statistical Society Series B* **79** 51-67.
- [19] PASSEMIER, D. and YAO, J. (2012). On determining the number of spikes in a high-dimensional spiked population model. *Rand. Matr. Theor. Appl.* **1** article 1150002.
- [20] PASSEMIER, D. and YAO, J. (2014). Estimation of the number of spikes, possibly equal, in the high-dimensional case. *Journal of Multivariate Analysis* **127** 173–183.
- [21] TELATAR, E. (1999). Capacity of Multi-antenna Gaussian Channels. *European Transactions on Telecommunications* **10** 585-595.
- [22] WANG, B., WANG, H., ZHANG, L., ZHU, D., LIN, D. and WAN, S. (2019). A Data-Driven Method to Detect and Localize the Single-Phase Grounding Fault in Distribution Network Based on Synchronized Phasor Measurement. *EURASIP J. Wirel. Commun. Netw.* **2019** 1–13.
- [23] WANG, Q. and YAO, J. (2017). Extreme eigenvalues of large-dimensional

- spiked Fisher matrices with application. *The Annals of Statistics* **45** 415 – 460.
- [24] ZENG, Y. and ZHU, L. (2022). Order Determination for Spiked Type Models. *Statistica Sinica* 1633-1659.
- [25] ZENG, Y. and ZHU, L. (2023). Order determination for spiked-type models with a divergent number of spikes. *Computational Statistics & Data Analysis* 107704.
- [26] ZHENG, K., GENG, Z., WANG, H., MA, F. and ZHANG, G. (2019). Single-phase Grounding Fault Detection and Localization based on Big Data From Synchronized Phasor Measurement. *Power System and Clean Energy* **36** 50–56.
- [27] ZHENG, S. (2012). Central limit theorems for linear spectral statistics of large dimensional F-matrices. *Annales de l'Institut Henri Poincaré, Probabilités et Statistiques* **48** 444 -476.
- [28] ZHENG, S., BAI, Z. and YAO, J. (2017). CLT for eigenvalue statistics of large-dimensional general Fisher matrices with applications. *Bernoulli* **23** 1130-1178.